



**Numerical modeling and sensitivity analysis of seawater  
intrusion in a dual-permeability coastal karst aquifer with  
5 conduit networks**

Zexuan Xu<sup>1,\*</sup>, Bill X. Hu<sup>2</sup> and Ming Ye<sup>3</sup>

10 <sup>1</sup>Climate and Ecosystem Sciences Division, Lawrence Berkeley National Laboratory,  
Berkeley, California, 94720, USA

<sup>2</sup>Institute of Groundwater and Earth Sciences, Jinan University, Guangzhou, Guangdong,  
China

<sup>3</sup>Department of Scientific Computing, Florida State University, Tallahassee, Florida,  
15 32306, USA

\*Corresponding author: email address: xuzexuan@gmail.com;

Submitted to Hydrology and Earth System Sciences

20



## Abstract

In a coastal karst aquifer, seawater intrudes significantly landward through the highly permeable subsurface conduit system, and contaminates the groundwater resources in the porous medium. In this study, a two-dimensional coupled density-dependent flow and transport SEAWAT model is developed to study seawater intrusion in the dual-permeability karst aquifer. To provide guideline for modeling seawater intrusion in such an aquifer, local and global sensitivity analysis are conducted to evaluate the parameters of boundary conditions and hydrological characteristics, including hydraulic conductivity, effective porosity, specific storage and dispersivity of the conduit and the porous medium. In the local sensitivity analysis, simulations are more sensitive to all parameters at the seawater and freshwater mixing zone than elsewhere. The most important parameter for simulations in both domains is salinity at the submarine spring, which is also the boundary condition of the conduit. The hydrological characteristics of the conduit network are not only important to the simulations in the conduit, but also significantly affect the simulations in the porous medium, due to the interactions between the two systems. Therefore, salinity and head observations in the conduits and karst features have more values for calibrating the models and understanding seawater intrusion in a coastal karst aquifer. Compared to the local sensitivity analysis, the global sensitivity results are different in several parameters (hydraulic conductivity, porosity and the boundary conditions at the submarine spring), mainly due to the non-linear relationship of the parameters with respect to the simulations. The results of global sensitivity analysis also indicate that the Darcy's equation does not accurately calculate the conduit flow rate with hydraulic conductivity



in the continuum SEAWAT model. Dispersivity is no longer an important parameter in  
45 the advection-dominated transport aquifer system with conduit, compared to the  
sensitivity results in a homogeneous porous medium. Based on the sensitivity analysis,  
the extents of seawater intrusion are quantitatively evaluated with the identified important  
parameters, including salinity at the submarine spring with rainfall recharge, sea level rise  
and longer simulation time under an extended low rainfall period.



50

Key Words: Seawater intrusion; Coastal karst aquifer; Variable-density numerical model;  
Dual-permeability karst system; Sensitivity analysis



## 1. Introduction




55 Many serious environmental ~~issues~~ have been caused by seawater intrusion in the  
coastal regions, such as soil salinization, marine and estuarine ecological changes, and  
groundwater contamination (Bear, 1999). Groundwater salinization is the primary  
detrimental effect of seawater intrusion to groundwater resources, since mixing with less  
than 1% of seawater (250 mg/L chloride) by volume makes freshwater non-potable  
60 (WHO, 2011). Custodio (1987) and Shoemaker (2004) summarized the controlling  
factors of seawater intrusion into a coastal aquifer, including the geologic and lithological  
heterogeneity, localized surface recharge, paleo-hydrogeological conditions and  
anthropogenic influences. Werner et al. (2013) concluded that climate variations,  
groundwater pumping, and fluctuating sea levels are important to the mixing of seawater  
65 and freshwater. On the other hand, sea level rise has been recognized as a serious  
environmental threat in this century (Voss and Souza, 1987; Bear, 1999; IPCC, 2007).





Sea level fluctuation has significant and complex impacts on seawater intrusion in a coastal aquifer under different conditions (Werner et al., 2013). The Ghyben-Herzberg relationship indicates that rising sea level causes extended seawater intrusion in a coastal aquifer, and significantly moves the mixing interface position further landward (Werner and Simmons, 2009). Essink et al. (2010) pointed out that seawater intrusion is exacerbated under sea level rise conditions in a large time scale due to global climate change. Likewise, high tides associated with hurricanes or tropical storms have been found to temporarily affect the extent of seawater intrusion in a coastal aquifer (Moore and Wilson, 2005; Wilson et al., 2011). However, tide fluctuation is ~~generally~~  ~~negatively~~  able to mixing interface movement over a regional and large time scale (Inouchi et al., 1990).

Modeling seawater intrusion in a coastal aquifer requires a coupled density-dependent flow and transport numerical model. In such model, **the solution of seawater**  is based on the groundwater velocity field from flow modeling, and salinity in turn determines water density and affects the simulation of flow field. Several variable-density numerical models have been developed and widely used, including SUTRA (Voss and Provost, 1984) and FEFLOW (Diersch, 2002). SEAWAT is a widely used density-dependent model, which solves flow equations by finite difference method, and transport equations by three major classes of numerical techniques (Guo and Langevin, 2002; Langevin et al., 2003). Generally speaking, most variable-density models are numerically complicated and computational expensive, because of the small timestep and the implicit procedure of solving flow and transport equations iteratively many times within each timestep (Werner et al., 2013).



Karst aquifers are particularly vulnerable to groundwater contamination including  
90 seawater intrusion in the coastal regions, since the well-developed sinkholes, karst  
windows, and subsurface conduit networks are highly permeable and usually connected.  
The caves are found directly open to the sea and become submarine springs below the sea  
level, connected with the conduit network as natural pathways for seawater intrusion. The  
highly permeable subsurface conduit network in a coastal karst aquifer cause seawater  
95 intrude significantly further landward and contaminate freshwater resources. The  
preferential flow within the conduit also significantly moves the position of seawater and  
freshwater mixing zone landward in karst aquifers (Calvache and Pulido-Bosch, 1997).  
Fleury et al. (2007) reviewed a number of studies about freshwater discharge and  
seawater intrusion through karst conduits and submarine springs in the coastal karst  
100 aquifers, and summarized some important controlling factors, including hydraulic  
gradient of equivalent freshwater head, hydraulic conductivity, and seasonal precipitation  
variation. Rainfall and regional freshwater recharges significantly affect the extents of  
seawater intrusion. Salinity near the outlet of conduit system is diluted by freshwater  
discharge during a rainfall season, but remains constant as saline water during a low  
105 rainfall period (Martin and Dean, 2001; Martin et al., 2012).

The Woodville Karst Plain (WKP) is a typical coastal karst aquifer, where the  
Spring Creek Springs (SCS) is a first magnitude spring consisting of 14 submarine  
springs located in the Gulf of Mexico (Fig. 1). SCS is also an outlet of the subsurface  
conduit network, exactly located at the shoreline beneath the sea level. Tracer test studies  
110 and cave diving investigations indicate that the conduit system starts from the submarine  
spring and extends 18 km landward connecting with an inland spring called Wakulla



Spring, although the exact locations of the subsurface conduits are unknown and difficult to explore (Kernagis et al., 2008; Kincaid and Werner, 2008). Some evidence shows that seawater intrusion has been observed through subsurface conduit system for more than 18  
115 km in the WKP (Xu et al., 2016). The relationship of seawater intrusion, groundwater flow and rainfall recharges in the WKP was described by a conceptual model of groundwater flow cycling in Davis and Verdi (2014), and then quantitatively simulated by a CFPv2 model in Xu et al. (2015b). In addition, Davis and Verdi (2014) also point out that sea level rise at the Gulf of Mexico in the past century could be a reason for the  
120 increasing discharge at an inland karst spring (Wakulla Spring) and decreasing discharge at SCS, when the hydraulic gradient towards the Gulf between the two springs decreases. (Insert Fig. 1 here)

Modeling groundwater flow in a dual-permeability karst aquifer is challenging, because of the non-laminar flow calculation in a karst conduit system (Davis, 1996;  
125 Shoemaker et al., 2008; Gallegos et al., 2013). Several coupled discrete-continuum numerical models have been developed and applied to solve the non-laminar flow in the conduit and the Darcian flow in a porous medium simultaneously, such as MODFLOW-CFPM1 (Shoemaker et al., 2008) and CFPv2 (Reimann et al., 2014; Reimann et al., 2013; Xu et al., 2015a; Xu et al., 2015b). However, these models only solve constant density  
130 governing equations, which are not applicable for simulating the density-dependent seawater intrusion processes in a coastal aquifer. The VDFST-CFP developed by Xu and Hu (2017) is a density-dependent discrete-continuum modeling approach to study seawater intrusion in a coastal karst aquifer with conduits, however, is only able to simulate synthetic cases but not yet for the field scale applications. Therefore, the



135 variable-density SEAWAT model is still used in this study, in which Darcy equation is not only used to calculate flow rate in the porous medium, but also the conduit flow rate with large values of hydraulic conductivity and effective porosity.

Very few studies addressed the parameter sensitivities of seawater intrusion in a coastal karst aquifer. Shoemaker (2004) performed a sensitivity analysis of the SEAWAT  
140 model for seawater intrusion in a homogeneous aquifer with porous medium, and concluded that dispersivity is an important parameter to the head, salinity and groundwater flow simulations and observations in transition zone. Shoemaker (2004) also concluded that salinity observations are more effective than head observation, and the “toe” of the transition zone is the most effective location for head and salinity simulations  
145 and observations. The sensitivity results in this study confirms some conclusions in Shoemaker (2004), and highlights the significance of conduit network in simulating seawater intrusion in a coastal karst aquifer, mainly due to the interaction between the karst conduit and the porous medium.

In this study, the local and global sensitivity analyses are conducted to evaluate  
150 the head and salinity simulations with respect to parameters in a coupled density-dependent flow and transport model. To our knowledge, this is the first attempt to assess the parameter sensitivities for seawater intrusion in a vulnerable dual-permeability karst aquifer with conduit network. The rest of the paper is arranged as follows: the details of local and global sensitivity analysis are introduced in Sect. 2. The model setup,  
155 hydrological conditions, model discretization, initial and boundary conditions are discussed in Sect. 3. The results of local and global sensitivity analysis are discussed in



Sect. 4. The scenarios of seawater intrusion simulation with different boundary conditions and elapsed time are presented in Sect. 5. The conclusions are made in Sect. 6.



## 160 2. Methods

The governing equations solved in the SEAWAT model can be found in the Guo and Langevin (2002), including the variable-density flow equation with additional density terms, and advection dispersion solute transport equation. The local and global sensitivity methods used in this study are briefly introduced below.

165

### 2.1 Local sensitivity analysis

In this study, UCODE\_2005 (Poeter and Hill, 1998) is applied in the local sensitivity analysis, which evaluates the derivatives of model simulations with respect to parameters at the specified values (Hill and Tiedeman, 2006). The forward difference approximation of sensitivity is calculated as the derivative of the  $i$ th simulation respect to the  $j$ th model parameters,

170

$$\frac{\partial y'_i}{\partial x_j} \Big|_b \approx \frac{y'_i(x + \Delta x) - y'_i(x)}{\Delta x_j} \quad 1)$$

where  $y'_i$  is the value of the  $i$ th simulation;  $x_j$  is the  $j$ th estimated parameter;  $x$  is a vector of the specified values of estimated parameter;  $\Delta x$  is a vector of zeros except that the  $j$ th parameter equals  $\Delta x_j$ .

175

The sensitivities are calculated by running the model once using the parameter values in  $x$  to obtain  $y'_i(x)$ , and then changing the  $j$ th parameter value and running the model again in  $x + \Delta x$  to obtain  $y'_i(x + \Delta x)$ . Scaled sensitivities are used to compare the





parameters sensitivities that may have different units. In UCODE\_2005, a scaling method is used to calculate the dimensionless scaled sensitivities (DSS) by the following equation,

$$dss_{ij} = \left( \frac{\partial y'_i}{\partial x_j} \right) \bigg|_x |x_j| \omega_{ii}^{1/2} \quad 2)$$

180 where  $dss_{ij}$  is the dimensionless scaled sensitivity of the  $i$ th simulation with respect to the  $j$ th parameter;  $\omega_{ii}$  is the weight of the  $i$ th simulation.

The DSS values of different simulations with respect to each parameter are accumulated as the composite scaled sensitivities (CSS). The CSS of the  $j$ th parameter is evaluated via:

$$css_j = \sum_{i=1}^{ND} \left[ (dss_{ij})^2 \bigg|_x / ND \right]^{1/2} \quad 3)$$

185 where  $ND$  is the number of simulated quantities, for example, the head and salinity simulations in this study.


## 2.2 Morris method in global sensitivity analysis

The local sensitivity analysis is conceptually straightforward and easy to compute  
190 without expensive computational cost. However, the sensitivity indices for parameters are calculated at the specified values only, but not for the entire parameter ranges. In addition, the indices are approximated in the first order derivative only, assuming a linear relationship of simulated quantities with respect to parameters. The higher orders relationship and interactions among parameters are not considered in the local sensitivity  
195 analysis.



The global sensitivity analysis evaluates the simulations with respect to parameters within the entire parameter range, instead of the specified values in the local sensitivity analysis. Morris method is applied to evaluate the global parameter sensitivities in this study (Morris, 1991). It is a so-called “one-step-at-a-time” method (OAT), meaning that



200 only one input parameter is perturbed and given a new value in each run. The Morris method is made by a number  $r$  of local changes at different points of the possible range of input values. In each parameter, a discrete number of values called levels are chosen with the parameter ranges of variation. Two sensitivity measures are proposed by Morris method for each parameter: the mean  $\mu$  that estimates the overall effect of the factor on  
 205 the output, and the standard deviation  $\sigma$  that estimates the ensemble of the second or higher-order effects (Saltelli et al., 2004). The mean  $\mu$  and standard deviation  $\sigma$  of the  
 EEs are evaluated with the  $r$  independent random paths in the Morris method,

$$\mu = \sum_{i=1}^r d_i / r \quad 4)$$

$$\sigma = \sqrt{\sum_{i=1}^r (d_i - \mu)^2 / r} \quad 5)$$

The  $k$ -dimensional vector  $x$  of the model parameters has components  $x_i$ , which can  
 210 be divided into  $p$  uniform intervals. The effect of changing one parameter at a time is evaluated in turn by the elementary effect (EE),  $d_i$ , which is defined as,

$$d_i = \frac{1}{\tau_y} \frac{[y(x_1^*, \dots, x_{i-1}^*, x_i^* + \Delta, x_{i+1}^*, \dots, x_k^*) - y(x_1^*, \dots, x_k^*)]}{\Delta} \quad 6)$$



where  $\Delta$  is the relative distance in the coordinate;  $\tau_y$  is the output scaling factor;  $\{x_i^*\}$  is the parameter set selected by different sampling method.

To compute the EE for the  $k$  parameters,  $(k+1)$  simulations are needed in the same  
215 way as local sensitivity method for the perturbation of each parameter, which is called one “path” (Saltelli et al., 2004). An ensemble of EEs for each parameter is generated by multiple paths of randomly generated parameter set. The total number of calculation is  $r(k+1)$  when Monte Carlo random sampling is applied, where  $r$  is the number of paths.

However, the global sensitivity analysis of this study does not apply Monte Carlo  
220 random sampling, which needs extremely large numbers ( $>250$ ) of paths to be generated for 11 parameters. The program takes very long time to complete the random sampling and sensitivity computation without parallelization. To save the running time and computational cost but obtain reliable result, the trajectory sampling is developed by Saltelli et al. (2004) and becomes a widely-used method to generate the ensembles of EEs  
225 for Morris method in the global sensitivity analysis. The definition of  $p$ -level is the same as Monte Carlo sampling, where  $\Delta = \pm p/[2(p-1)]$ , either positive or negative. The trajectory method starts by randomly selecting a “base” value  $x^*$  for the vector  $x$ . Each component  $x_i$  of  $x^*$  is sampled from the set  $(0, 1/(p-1), 2/(p-1), \dots, 1)$ . The randomly selected vector  $x^*$  is used to generate the other sampling points but not one of them,  
230 which means that the model is never evaluated at vector  $x^*$ . The first sampling point,  $x^{(1)}$ , is obtained by changing one or more components of  $x^*$  by  $\Delta$ . The choice of components  $x^*$  to be increased or decreased is conditioned by that  $x^{(1)}$  still being within the domain. The second sampling point,  $x^{(2)}$ , is generated from  $x^*$  with the property that it differs



from  $x^{(1)}$  in its  $i$ th component, which has been either increased or decreased by  $\Delta$ , but  
235 also still being within the domain. The third sampling point,  $x^{(3)}$ , differs from  $x^{(2)}$  for  
only one component  $j$ , for any  $j \neq i$ , will be  $x_j^{(3)} = x_j^{(2)} + \Delta$ . A succession of  $(k+1)$   
sampling points  $x^{(1)}, x^{(2)}, \dots, x^{(k+1)}$  is produced in the input parameters space called a  
trajectory, with the key characteristic that two consecutive points differ in only one  
component. As a result, any component  $i$  of the ‘base’ vector  $x^*$  has been selected at least  
240 once by  $\Delta$  in order to calculate one EE for each parameter.

Once a trajectory is constructed and evaluated by Morris method, an EE for each  
parameter  $i$ ,  $i = 1, \dots, k$ , can be computed. If  $x^{(l)}$  and  $x^{(l+1)}$ , with  $l$  in the set in  $(1, \dots, k)$ ,  
are two sampling points differing in their  $i$ th component, the EEs associated with the  
parameter  $i$  is,

$$d_i(x^{(l)}) = \frac{[y(x^{(l+1)}) - y(x^{(l)})]}{\Delta}, \quad 7)$$

245 A random sample of  $r$  EEs is selected at the beginning of sampling. Each  
trajectory sampling has a different starting point that is randomly generated. The points  
belonging to the same trajectory are not independent, but the  $r$  points sampled from each  
distribution belonging to different trajectories are independent.

### 3. Model development

250 In this study, a two-dimensional SEAWAT model is setup to simulate seawater  
intrusion through the major subsurface conduit network in the Woodville Karst Plain  
(WKP) (Fig. 1). Figure 2 presents a schematic figure of the cross section in a coastal karst  
aquifer with a conduit network and a submarine spring opening to the sea. The model  
spatial domain is not a straight line from the submarine Spring Creek Springs to Wakulla



255 Spring, but a cross section along the major conduit pathway of seawater intrusion in the coastal karst aquifer. The model spatial domain and geometry in this study is setup exactly as the regional scale in the field, for example, the 18 km long and 91 meters deep conduit network in the WKP.

(Insert Fig. 2 here)

260 However, this study only addresses the seawater intrusion through the conduit, and the flow and solute exchanges between the conduit and the surrounding porous medium within the cross section. In the field, seawater intrudes further landward through the conduit network and flows into the surrounding porous medium, in both the vertical and the horizontal direction that perpendicular to the cross section. The simulation of  
265 saltwater flow and transport in the perpendicular direction within the porous medium is beyond the scope of the model used in this study, which only aims to study seawater intrusion through the conduit and the porous medium of the cross section. This assumption of 2D model is reasonable, considering that the exchange fluxes from the conduit to the surrounding porous medium trivially affect the seawater intrusion through  
270 the channel, when the conduit wall exchange permeability is relatively smaller compared with the large permeability in the conduit. The simplified model is used in this study, since the main purpose of this study is to evaluate the role of subsurface conduit in seawater intrusion in the coastal karst aquifer. In addition, most SEAWAT models are setup for 2D cross section with high-resolution vertical discretization. 3D coupled  
275 density-dependent flow and transport model is rarely seen, due to the constraint of computational cost. The parameter sensitivities of 3D density-dependent numerical model are even more difficult to be evaluated within a reasonable time frame, because running



the model many times with parameters perturbation are required in the sensitivities analysis.



280

### 3.1 Hydrological conditions

Table 1 presents the hydrological characteristics of the Upper Floridan Aquifer (UFA) in the WKP. The parameter values are evaluated in the following local sensitivity analysis and applied in the seawater intrusion scenarios in Sect. 5. These parameters have  
285 been calibrated in the regional-scale groundwater flow and solute transport models by Davis et al. (2010), and have been applied in many previous modeling studies (Gallegos et al., 2013; Xu et al., 2015a; Xu et al., 2015b). This study does not aim to re-calibrate the model, since observation data in the field are insufficient, especially in the subsurface conduit. The head and salinity measurements in the conduit are rarely available, due to  
290 the difficulties of subsurface conduit investigation and monitoring devices installation. (Insert Table 1 here)

The hydrological characteristics (hydraulic conductivity, specific storage and effective porosity) of the conduit system are generally greater than the surrounding porous medium. Hydraulic conductivity of the porous medium is assigned as 2286 m/day  
295 (7500 ft/day), and as large as 610,000 m/day (2,000,000 ft/day) for the conduit system. Even the hydraulic conductivity of porous medium in the study region is larger than most alluvial aquifers, because of the numerous small fractures and relatively large pores in a karst aquifer due to dissolution of carbonate rocks. Specific storage and effective porosity in the porous medium are assumed as  $5 \times 10^{-7}$  and 0.003, respectively. Specific storage  
300 and effective porosity are 0.005 and 0.300 in the conduit layer, respectively. The



longitudinal dispersivity is estimated as 10 m in the porous medium, but is assumed very small (0.3 m) in the conduit, because advection is dominated and dispersion is negligible in the solution of transport in the conduit.

### 305 **3.2 Spatial and temporal discretization**

The grid discretization and boundary conditions of the two-dimensional SEAWAT numerical model are shown in Fig. 3, which consists of 140 columns and 37 layers in the cross section. Guo and Langevin (2002); Werner et al. (2013) pointed out that higher-resolution grid discretization in the vertical direction is required for modeling  
310 the density-dependent flow. The vertical thickness of each cell is set uniformly as 3.048 m (10 ft) in this study, with significantly higher resolution than the 152 m (500 ft) thickness in many previous constant-density modeling studies in the WKP, for example, Davis and Katz (2007); Davis et al. (2010); Xu et al. (2015a); Gallegos et al. (2013); Xu et al. (2015b).

315 (Insert Fig. 3 here)

The horizontal dimension for each cell is set uniformly 152 m (500 ft) as the  
scales in the field, except columns #22 and #139, which are 15.2 m (50 ft) as the vertical conduit network connecting the submarine spring (SCS) and inland spring (Wakulla Spring), respectively. The sizes of spring outlets and the conduit are based on the  
320 observations data in the field and the calibrated models in previous studies (Gallegos et al., 2013). However, the diameter of horizontal conduit network is assumed homogeneous in this study. The outlet of vertical conduit system is the submarine spring (SCS) located at the shoreline at column #22. The conduit system starts from the





submarine spring, descends downward to layer #29 (nearly 100 m below sea level),  
325 horizontally extends nearly 18 km from column #22 to column #139, and then rises  
upward to the top through column #139. Seawater intrudes at the SCS on the first layer of  
column #22, and then flows vertically downward into the conduit system. The inland  
spring is simulated by the DRAIN package as general head boundary condition in the  
SEAWAT model. All layers are simulated as confined aquifer since the conduit is fully  
330 saturated, which are identical to the previous numerical models used in Davis et al.  
(2010); Xu et al. (2015a); Xu et al. (2015b) in the WKP.

In this study, a transient 7-day stress is simulated in the SEAWAT model. The  
scenarios of longer simulation time are exceptions for evaluating seawater intrusion  
under an extended low rainfall period in Sect. 5.4. The timestep of flow model is set as  
335 0.1 days, and the timestep of transport model is determined by SEAWAT automatically.

### 3.3 Initial and boundary conditions

The initial condition of head is set 0.0 m as the present-day sea level for the cells  
from the left boundary to the shoreline (column #22), and gradually rises to 1.52 m (5.0  
340 ft) at inland boundary on the right, based on the elevation of the inland spring. Please  
note that values of head are written in the input files of SEAWAT model, instead of  
equivalent freshwater head. The initial conditions of salinity are assumed constant along  
the vertical direction in each column. Salinity at the leftmost 10 columns is set uniformly  
as 35.0 PSU (Practical Salinity Unit) as seawater without mixing near the sea boundary.  
345 The seawater/freshwater mixing zone has the salinity initial condition from 35 PSU at  
column #11 to 0 PSU at column #45, with a gradient of 1.0 PSU per column. Salinity is





set uniformly as 0.0 PSU from column #46 to the inland boundary on the right, as uncontaminated freshwater before seawater intrudes. Several testing cases have been made to test and confirm that the initial conditions trivially affect the modeling results.

350 The boundary conditions are also presented in Fig. 3. The bottom of model domain is no-flow boundary condition as the less-permeable confining unit of the UFA base. The constant head and concentration inland boundary condition on the right is 1.5 m (5.0 ft) as the elevation of inland spring, and 0.0 PSU as uncontaminated freshwater. The seawater boundary on the left is 3.38 km away from the shoreline, set as 0.0 m  
355 constant head as the present-day sea level and 35.0 PSU constant concentration as seawater without mixing. However, the boundary conditions of head and salinity at the submarine spring (column #22, layer #1) are adjusted and evaluated in the scenarios of different sea level, salinity and rainfall conditions in Sect. 5.



#### 360 4. Sensitivity Analysis

Sensitivity analysis evaluates the uncertainties of salinity and head simulations with respect to eleven parameters, provides the knowledge for understanding the hydrological characteristics and boundary conditions in a coastal karst aquifer with a conduit. The symbols and definitions of the eleven parameters in the SEWAT model are  
365 listed in Table 1, as well as the specified evaluated values in local sensitivity analysis, and the parameter ranges in the global sensitivity analysis (Table 1). There are six parameters in the groundwater flow model, including hydraulic conductivity (HY\_P and HY\_C), specific storage (SS\_P and SS\_C) of the conduit and the porous medium, recharge rate (RCH) and the sea level at the submarine spring (H\_SL). The other five





370 parameters, including effective porosity (PO\_P and PO\_C), dispersivity (DISP\_P and  
DISP\_C) of the conduit and the porous medium, and the salinity at the submarine spring  
(SC), are in the solute transport model.

#### 4.1 Local sensitivity analysis

375 In the local sensitivity analysis, the CSS (composited scaled sensitivities) of  
parameters with respect to head and salinity simulations are calculated at several  
locations in the conduit and the porous medium domains. Again, the specified parameter  
values in the local sensitivity analysis are consistent with the hydrological characteristics  
of the UFA, and the head and salinity boundary conditions of the conduit outlet are set as  
380 present-day sea level and seawater without mixing. The simulation results with the  
parameters in the local sensitivity analysis are presented in Sect. 5.1, as the maximum  
seawater intrusion case. Parameter sensitivities are computed at several locations, from  
column #25 to column #75 with an interval of 5 cells along the horizontal conduit (layer  
#29), where column #25 is very close to the shoreline and column #75 is basically the  
385 uncontaminated freshwater aquifer. The parameter sensitivities of simulations in a porous  
medium are evaluated at layer #24, 15.2 m (50 ft) or 5 layers above the conduit layer,  
from column #25 to column #75 with an interval of 5 cells along the horizontal direction.

##### 4.1.1 Local sensitivity analysis of simulations in the conduit

390 Figure 4 shows the arithmetic mean of CSS for each parameter with respect to  
simulations in all evaluated locations along the conduit layer. The largest CSS value in  
the local sensitivity analysis indicates that salinity at the submarine spring (SC) is the



most important parameter to both salinity and head simulations. Hydraulic conductivity,  
specific storage and effective porosity of the conduit (HY\_C, SS\_C and PO\_C) as well as  
395 sea level at the submarine spring (H\_SL) are also important parameters. Hydraulic  
conductivity, specific storage and effective porosity of the porous medium (HY\_P, SS\_P  
and PO\_P), recharge rate (RCH) and dispersivity (DISP\_C and DISP\_P) are the less  
important parameters. Generally speaking, the parameter sensitivities with respect to head  
simulations are similar and consistent with salinity simulations.

400 (Insert Fig. 4 here)

Salinity at the submarine spring (SC) is the most important parameter, because the  
submarine spring is the boundary condition and the major source of seawater intrusion  
through the conduit network in a coastal karst aquifer. Seawater enters the conduit system  
at the submarine spring, and continuously intrudes landward through the subsurface  
405 conduit system. Seawater also flows into the surrounding porous medium via the  
exchanges between the two domains, when the equivalent freshwater head in the conduit  
is larger than the surrounding porous medium. Increasing salinity at the submarine spring  
causes further seawater intrusion through the conduit network with higher equivalent  
freshwater head, moves the mixing zone position further landward, and vice versa. The  
410 salinity at the submarine spring is determined by freshwater mixing and dilution from the  
conduit network, in other words, is controlled by the rainfall recharges and freshwater  
discharge from the aquifer to the sea. In other word, freshwater dilution is represented by  
salinity at submarine study instead of the recharge flux on the boundary, which is  
unknown and difficult to quantitatively estimate in a two-dimensional numerical model  
415 In addition, the simulations in the conduit are more sensitive to hydraulic conductivity,



specific storage and effective porosity of the conduit (HY\_C, SS\_C and PO\_C) rather than the hydrological characteristics of the porous medium (HY\_P, SS\_P and PO\_P), since conduit network is the major pathway for seawater intrusion. The sea level at the submarine spring (H\_SL) is indicated as an important boundary condition in the model, but is not as important as the salinity at the submarine spring (SC). In other words, the extent of seawater intrusion in the conduit is more sensitive to rainfall recharge and freshwater discharge that represented by the parameter SC, rather than the sea level and/or tide level variations. Recharge (RCH) is not an important parameter with respect to simulation in this study, which only represents a small portion of total rainfall recharge in the two-dimensional seawater intrusion model, since the rainfall recharges in the whole springshed converge into the subsurface conduit. In this study, salinity at the submarine spring represents the rainfall recharge with the largest CSS value, instead of the parameter RCH.

In the local sensitivity analysis, the conduit and porous medium dispersivities (DISP\_C and DISP\_P) are not important to salinity and head simulations, because advection is dominated in the transport of seawater within the highly permeable conduit network, while dispersion is negligible in such rapid flow condition. This is different from the results of parameter sensitivities in a homogeneous aquifer, where dispersivity is actually a very important parameter. Meanwhile, the dispersion solution and dispersivity sensitivities are hardly calculated when conduit flow becomes turbulent. On the other hand, the numerical dispersion is significantly greater than the solution of dispersion equation in the conduit. The Peclet number can be as great as 2500, which is obviously beyond the Peclet number criteria ( $<4$ ) for solving the advection dispersion transport



equation by finite difference method. In other words, the calculation of salinity dispersion  
440 is inaccurate in the conduit by the SEAWAT model with large uncertainty, which brings  
about the inaccurate results of dispersivity sensitivities .

Six parameters with the largest CSS are presented in Fig. 5, with respect to the  
combination of head and salinity simulations in the evaluated locations along the conduit  
network, from column #25 to column #75. The largest CSS values for all parameters are  
445 found at either column #50 or #55 within the conduit, matches the position of  
seawater/freshwater mixing zone along the conduit network in the maximum seawater  
intrusion case in Sect. 5.1. The CSS values are relatively larger for all parameters at the  
mixing zone, because head and salinity simulations only change significantly near the  
mixing zone but remain constant in other locations.

450 (Insert Fig. 5 here)

#### 4.1.2 Local sensitivity analysis of simulations in the porous medium

Figure 6 shows the arithmetic mean of CSS for each parameter with respect to  
head and salinity simulations in all evaluated locations along the porous medium (layer  
455 #24). Similar to the parameter sensitivities of simulations in the conduit, the largest CSS  
indicates that salinity at the submarine spring (SC) is still the most important parameter  
with respect to simulations in the porous medium, although it is a boundary condition of  
the conduit system. However, some parameter sensitivities are different from the results  
of simulations in the conduit. The hydraulic conductivity and effective porosity of both  
460 the conduit and porous medium (HY\_C, HY\_P, PO\_C & PO\_P), specific storage of the  
conduit (SS\_C) and dispersivity of the porous medium (DISP\_P) have smaller CSS than



the parameter SC, but are still identified as relatively important parameters. The other parameters (DISP\_C, RCH and SS\_P) are not important to the simulations in the porous medium. The CSS of the eight relatively important parameters are plot at different  
465 evaluated locations along the layer of porous medium in Fig. 7. Similar to the sensitivity analysis of simulations in the conduit, the largest CSS of each parameter is found at either column #35 or #40, matches the mixing zone position in the porous medium in the maximum seawater intrusion case in Sect. 5.1.

(Insert Fig. 6 and 7 here)

470 Salinity at the submarine spring (SC) is still the most important parameter for simulations in the porous medium, because the submarine spring is the major source and the entrance of seawater intrusion into the aquifer. The conduit network is the major pathway for seawater intruding landward and flowing into the surrounding porous medium. Similarly, the conduit hydrological characteristics, such as hydraulic  
475 conductivity, effective porosity and specific storage (HY\_C, PO\_C and SS\_C), are also important parameters with respect to the simulations in the porous medium. Groundwater flow and seawater transport through the conduit system have significant impact on the head and salinity simulations in the surrounding porous medium. On the other hand, the hydrological characteristics of porous medium, including hydraulic conductivity,  
480 effective porosity and dispersivity (HY\_P, PO\_P and DISP\_P), also have large CSS with respect to simulations in the porous medium. It is easy to understand that head and salinity simulations are sensitive to the in-situ hydrological characteristics of porous medium. In summary, simulations in the porous medium are sensitive to the hydrological characteristics of both the conduit and the porous medium, indicating that the interaction



485 between the two domains are important for simulating seawater intrusion in a dual-  
permeability coastal karst aquifer. As a result, salinity and head observations in the  
conduits and other karst features have significant meanings and values for calibrating  
numerical models and for understanding seawater intrusion in a coastal karst aquifer.



#### 490 **4.2 Global sensitivity analysis**

The derivatives of head and salinity simulations with respect to the selected  
parameters are calculated to test if the CSS values in the local sensitivity analysis is  
representative for the entire parameter range (Fig. 8). For example, head and salinity  
simulations in the conduit are nearly constant to the dispersivity of the porous medium  
495 (DISP\_P), which is evaluated as an unimportant parameter in the local sensitivity study.  
Simulation in the porous medium shows a linear relationship to the parameter HY\_P,  
with a median level CSS calculated in the local sensitivity analysis. However, both head  
and salinity simulations are non-linear to salinity at the submarine spring (SC), which is  
the most important parameter and the boundary condition of conduit system with the  
500 largest CSS (Fig. 8). The local sensitivity analysis is only based on the specified  
parameter value, but not representative for the entire parameter ranges and higher-order  
derivatives. Therefore, the global sensitivity analysis is necessary for fully evaluating the  
relationship of simulations with respect to parameters.

(Insert Fig. 8 here)

505 In the following global sensitivity analysis, parameter sensitivities with respect to  
simulations are calculated in a specified location in the conduit (column #50, layer 29)  
and the porous medium (column #35, layer #24), respectively. The parameters



sensitivities have the largest CSS in these locations, which are identical to the mixing zone position is in the maximum seawater intrusion case in Sect. 5.1. The Trajectory  
510 sampling method developed by Saltelli et al. (2004) is introduced in Sect. 2.2 and applied in this study, with the recommended choice of  $p = 4$  and  $r = 10$  by Saltelli et al. (2004).



### 5.2.1 Global sensitivity analysis to simulations in the conduit

In the global sensitivity analysis, the mean and standard deviation of the EEs for  
515 each parameter with respect to salinity simulation in the conduit (column #50, layer #29) are presented in Fig. 9a. The largest mean value indicates that parameter SC is the most important parameter to salinity simulations. It is consistent with the result in local sensitivity analysis, since the submarine spring is the boundary condition of the major pathway for seawater intrusion in the numerical model. The non-linear relationship of  
520 salinity simulation with respect to parameter SC shown in Fig.8 is the main reason for the largest standard deviation of the EEs, since the derivatives vary at different evaluated values. Similar to the local sensitivity analysis, the hydraulic conductivity and effective porosity of the conduit (HY\_C and PO\_C), as well as sea level (H\_SL), are all important to salinity simulation with relatively large mean and standard deviation values of EEs.  
525 These parameters are either the hydrological characteristics or the boundary conditions of conduit network. However, other parameters are relatively less important with small mean and standard deviation of EEs. Generally speaking, the global sensitivity study results for salinity simulation in the conduit are similar to the local sensitivity analysis.  
(Insert Fig. 9 here)





530           The global parameter sensitivities with respect to head simulation exhibit more complicated (Fig. 9b). The mean and standard deviation of EEs for each parameter with respect to head simulation are smaller than the sensitivities of salinity simulation, which means that salinity is more sensitive than head simulation with respect to the parameters. The mean values of EEs indicate that the specific storage (SS\_C) and effective porosity  
535 (PO\_C) of the conduit are the two most important parameters with respect to the head and salinity solutions in the coupled density-dependent flow and transport model, respectively. The values of specific storage and effective porosity are calculated by the percentage of void space in the aquifer, based on the physically measured data in the field. Although salinity at the submarine spring (SC) does not have the largest mean of EEs, it  
540 is still an important parameter for head simulation with a large standard deviation of EEs, since the derivatives vary in different evaluated locations, with non-linear relationship to head simulation (Fig. 8). Head simulations are also sensitive to the boundary conditions of salinity in the transport model, because equivalent freshwater head is a function of density in terms of salinity simultaneously in the coupled variable-density flow and  
545 transport model.

          The means and standard deviations of EEs for effective porosity and specific storage of the conduit (PO\_C and SS\_C) are much larger than hydraulic conductivity (HY\_C), indicating that head simulation in the conduit is more sensitive to effective porosity and specific storage, rather than the hydraulic conductivity. The sensitivity result  
550 is different from the common knowledge and empirical experience in hydrogeology, but is actually reasonable in karst modeling. The uncertainty of non-laminar flow rate calculation in the continuum model is highlighted in the sensitivity analysis. In the



SEAWAT model, the Darcy equation estimates the specific discharge in the whole model domain including the conduit system, however, is only accurate for laminar seepage flow  
555 in the porous medium. Groundwater flow easily becomes non-laminar and higher than the critical Reynolds number in the conduit system with giant diameter. In such case, the conduit flow rate is non-linear to head gradient and beyond the applicability of Darcy equation, which means that the Darcy equation in SEAWAT model has relatively large error in the non-laminar conduit flow calculation. As a result, the sensitivities of  
560 hydraulic conductivity have significant uncertainty to evaluate the permeability of conduit system under non-laminar flow condition.

### 5.2.2 Global sensitivity analysis of simulations in the porous medium

The means and standard deviations of EEs for each parameter with respect to  
565 salinity simulations in the porous medium are shown in Fig. 10a. The mean and standard deviation values indicate that parameters HY\_P and SC are the two most important parameters for simulations in the porous medium. Hydraulic conductivity of the porous medium (HY\_P) is an important term for solving head and groundwater seepage velocity in the flow equation, which then determines the advective velocity of transport equation  
570 in the porous medium. As the boundary condition of conduit system, salinity at the submarine spring (SC) is also important as the major source of seawater intrusion not only in the conduit system, but also in the surrounding porous medium via exchanges between the two domains. The global sensitivity analysis of parameter SC highlights the significance of the interaction between the conduit and the porous medium domains in a  
575 dual-permeability aquifer. However, salinity at the submarine spring (SC) with respect to



simulations in the porous medium has the largest CSS in the local sensitivity study, while the CSS of hydraulic conductivity of the porous medium (HY\_P) is much smaller (Fig. 6). Parameter sensitivity of salinity at submarine spring (SC) is evaluated at the specified value (35.0 PSU) with the largest derivative in the local sensitivity analysis (Fig. 8).

580 However, simulations are non-linear to the parameter SC with variable sensitivities. In other words, global sensitivity analysis provides more comprehensive knowledge of parameter sensitivities within the ranges. Sea level at the submarine spring (H\_SL) and effective porosity of the porous medium (PO\_P) are important parameters to salinity simulations as well. Similar to salinity at the submarine spring (SC), sea level (H\_SL) is  
585 the boundary condition of flow model in the conduit system, which has great impacts on head and salinity solutions in the surrounding porous medium via exchange between the two domains. The EEs of effective porosity and specific storage of the conduit (PO\_C and SS\_C) also have relatively large mean and standard deviation to salinity simulation in the porous medium, highlight the values of dynamic interaction between the conduit  
590 and the porous medium in this study.

(Insert Fig. 10 here)

On the other hand, the mean and standard deviation of EEs of parameters indicate that the matrix hydraulic conductivity (HY\_P) is the most important parameter for head simulation in the porous medium (Fig. 10b), as a common knowledge in groundwater  
595 modeling. Please note this is different from the global sensitivity results of simulations in the conduit, in which the EEs of effective porosity and specific storage of the conduit (PO\_C and SS\_C) have larger mean and standard deviation values than hydraulic conductivity (HY\_C), due to the significant uncertainty of conduit flow calculation in the



continuum SEAWAT model. Although not as significant as parameter HY\_C, effective  
600 porosity of the porous medium (PO\_P) is an important parameter with relatively large  
mean and standard deviation of EEs, because equivalent freshwater head is calculated by  
water density in terms of salinity in the coupled flow and transport model. On the other  
hand, sea level at the submarine spring (H\_SL) is also an important parameter with  
respect to head simulation in the porous medium. As the boundary condition of the  
605 conduit, parameter H\_SL affects head solutions in the surrounding porous medium by  
determining the head-dependent exchange flux between the two domains. In general, the  
boundary conditions (SC and H\_SL) and hydrological properties (SS\_C, HY\_C and  
PO\_C) of the conduit system have great impacts on head simulations in the porous  
medium.

610 Both local and global sensitivity analysis highlight that field observations and  
numerical simulations of the karst features, including the boundary conditions and  
hydrological characteristics of sinkholes, karst windows and subsurface conduit system,  
are important to model uncertainty analysis. Simulations in the porous medium are  
sensitive to hydrological characteristics and boundary conditions of the conduit,  
615 indicating the significance of conduit system on modeling seawater intrusion in a dual-  
permeability karst aquifer. The conduit system serves as the major pathway for seawater  
intrusion further landward and groundwater contamination in the aquifer. On the other  
hand, dispersivity is no longer an important parameter in this study, compared with the  
sensitivity analysis in Shoemaker (2004) that dispersivity is found as an important  
620 parameter, in which a homogeneous porous medium domain is evaluated without the  
preferential advective flow. In a dual-permeability karst aquifer system, advection



transport is dominated in the conduit and the surrounding porous medium as well, while dispersion becomes relatively less important. In this study, the uncertainty of dispersivity sensitivities can be significant, since the large Peclet number in the conduit is beyond its  
625 criteria for solving transport equation by finite difference method. An experiment of inactivating DSP package in SEAWAT confirms that the mixing is mostly due to the numerical dispersion instead of the solution of dispersion equation in this study.

In general, parameter sensitivities of simulations in the porous medium are more complicated than those in the conduit, especially for the head simulations. The global  
630 sensitivity analysis provides an insight of the parameter interactions and the higher-order relationship with respect to simulations.



## 5. Seawater Intrusions in Scenarios



Sensitivity analysis finds that salinity at the submarine spring (SC) is the most  
635 important parameter with respect to head and salinity simulations in both the conduit and the porous medium. Sea level at the submarine spring (H\_SL) is the other important boundary condition of the conduit system in the SEAWAT model. The hydrological conditions of the aquifer are represented by these two boundary conditions, such as rainfall and regional freshwater recharges (SC), and the sea/tide level at the submarine  
640 spring (H\_SL). In order to evaluate the impacts of boundary conditions on seawater intrusion in a dual-permeability system, the extents of seawater intrusion under scenarios of boundary conditions are simulated by the SEAWAT model and quantitatively measured. In addition, the length of elapsed time in simulation is constant in the sensitivity analysis for consistent comparison purposes. The extents of seawater intrusion



645 in a coastal karst aquifer during an extended low rainfall periods are evaluated by  
extending the elapsed time in simulation in Sect. 5.4. In each scenario, only one  
parameter is adjusted and others remain the same as the original values in the maximum  
seawater intrusion case.

### 650 **5.1 The maximum seawater intrusion case**

The head and salinity boundary conditions at the submarine spring are set as 0.0  
m as the present-day sea level, and 35.0 PSU as seawater without mixing filled in the  
conduit system outlet, respectively. In the local sensitivity analysis, parameter  
sensitivities are evaluated at the specified parameter values in this case. This case is  
655 called the maximum seawater intrusion case, in which the longest distance of seawater  
intrusion is simulated by assuming that freshwater dilution by rainfall recharge is  
negligible in the entire aquifer, and the outlet of conduit system is filled with seawater  
without mixing. Figure 11 presents the salinity and head simulations in the cross section  
with a 7-day simulation. This case is also set as the benchmark for the following  
660 scenarios.

(Insert Fig. 11 here)

According to the Ghyben-Herzberg relationship, high-density seawater intrudes  
landward through the deep aquifer beneath the freshwater flowing seaward on the top.  
The equivalent freshwater head at the submarine spring is calculated as 2.29 m (7.5 ft)  
665 when salinity is 35.0 PSU at the submarine spring, and seawater without mixing is filled  
with the 91 meters deep submarine cave of the conduit. The equivalent freshwater head is  
higher than the 1.52 m (5.0 ft) constant head at the inland spring, diverts the hydraulic



gradient landward and causes seawater to intrude into the aquifer. Seawater moves significantly further landward through the highly permeable conduit network, also  
670 gradually intrudes landward in the surrounding porous medium via exchange on the conduit wall. The position of seawater/freshwater mixing zone in the deep porous medium beneath the conduit is only slightly behind the seawater front in the conduit, because high-density saline water easily moves downward from the conduit into the deeper aquifer. The area with relatively smaller salinity to the left of the vertical conduit  
675 network near the shoreline is due to the freshwater discharge dilution from the aquifer to the sea, since the equivalent freshwater head only increases at the submarine spring but remains constant as 0 m in other areas. Simulation result shows that the mixing zone position in the conduit, defined as the location with salinity of 5.0 PSU, reaches nearly 5.80 km landward from the shoreline. The width of mixing interface, defined as the  
680 distance between the locations with salinity of 1.0 PSU and 25.0 PSU, is about 7 grid cells or 1.13 km (0.7 miles) in both the conduit and porous medium.

## 5.2 Salinity variation at the submarine spring (SC)

Sensitivity analysis indicates that the salinity at the submarine spring (SC) is  
685 generally the most important parameter with respect to simulations in both the conduit and the porous medium. In this study, rainfall and regional freshwater recharges are simulated by salinity at the submarine spring instead of time-variable flux on the boundary condition. Salinity at the submarine spring is diluted by large amount of rainfall recharge and freshwater discharge after a significant precipitation event, but remains high  
690 after an extended low rainfall period as the maximum seawater intrusion case in Sect. 5.1.



The equivalent freshwater head at the submarine spring is calculated as 2.29 m (7.5 ft) when seawater without mixing is filled with the conduit system, however, proportionally decreases with the salinity at the submarine spring to 0.0 m, when salinity is 0.0 PSU and freshwater is filled with the conduit system. The impact of freshwater recharge on

695 seawater intrusion is evaluated in four scenarios with different salinity at the submarine spring of 0.0 PSU, 10.0 PSU, 20.0 PSU and 30.0 PSU. The head boundary condition is kept constant as 0.0 m as present-day sea level (Fig. 12). The mixing zone positions in both the conduit and porous medium are located at 4.0 (4.5) km away from the shoreline in the cases of salinity of 10.0 (20.0) PSU at the submarine spring. Rainfall recharge and

700 freshwater discharge move the interface significantly seaward. In addition, the mixing zone is very close to the shoreline in the case of salinity of 0.0 PSU at the submarine spring, when seawater intrusion is suspended and blocked by large amount of freshwater dilution. The shape of mixing interface is similar to the maximum seawater intrusion benchmark. However, the width of mixing interface is much wider due to the smaller or

705 even reversed hydraulic gradient from the aquifer to the sea. In such scenarios, the solution of dispersion equation is more important in salinity simulation with slower groundwater seepage flow. Generally speaking, seawater no longer intrudes significantly inland after a heavy rainfall event, and the mixing interface moves seaward when freshwater dilutes the salinity at the submarine spring and the conduit network.

710 (Insert Fig. 12 here)





### 5.3 Sea level variation at the submarine spring (H\_SL)

Sensitivity analysis indicates that sea level at the submarine spring is also an important parameter. Approximate 1.0 m sea level rise at the beginning of next century is predicted by IPCC (2007), with significant impacts on seawater intrusion in a coastal karst aquifer. The extents of seawater intrusion in the conduit and porous medium under 0.91 m (3.0 ft) and 1.82 m (6.0 ft) sea level rise conditions are quantitatively evaluated in this study (Fig. 13). Salinity at the submarine spring remains 35.0 PSU as same as the maximum seawater intrusion benchmark, but the head at the submarine spring increases to 0.91 m (3.0 ft) and 1.82 m (6.0 ft) as rising sea level, respectively. The width and shape of the mixing zone are similar to the simulation result in the maximum seawater intrusion benchmark. However, the mixing zone position moves landward in the conduit at almost 7.08 km from the shoreline when sea level rises 0.91 m (3.0 ft), which is 1.28 km further inland than the simulation with the present-day sea level. In the other extreme case of 1.82 m (6.0 ft) sea level rise, seawater intrudes additional 0.97 km further inland along the conduit than the case with 0.91 m (3.0 ft) sea level rise, or 2.25 km further inland than the simulation with present-day sea level. Compared with a homogeneous aquifer, seawater intrudes further landward through the conduit network in such a dual-permeability aquifer. The modeling of sea level rise confirm the concerns of severe seawater intrusion in the coastal region, also highlight the impacts on a karst aquifer with conduit system as the major pathway for seawater intrusion. In addition, sea level rise influence the regional flow field and hydrological conditions in a coastal aquifer. In Davis and Verdi (2014), increasing groundwater discharge at the inland Wakulla Spring in the WKP was observed associated with sea level rise in the past decades. The



735 relationship between spring discharge and sea level was quantitatively simulated by a  
CFPv2 numerical model in Xu et al. (2015b). However, the changes of flow field and  
hydrological conditions are not addressed and simulated in this study  
(Insert Fig. 13 here)

#### 740 **5.4 Extended low rainfall period**

The extents of seawater intrusion under scenarios of extended low rainfall periods  
are presented in Fig. 14, although the elapsed time in simulation is not evaluated in the  
sensitivity analysis. The simulated time period is extended to 14, 21 and 28 days, with the  
conditions of salinity and sea level at the submarine spring as 35.0 PSU and 0.0 m,  
745 respectively, as same as the maximum seawater intrusion benchmark.  
(Insert Fig. 14 here)

During an extended low rainfall period, seawater intrudes through both the  
conduit and the porous medium domains with time, since the 2.29 m (7.5 ft) equivalent  
freshwater head at the submarine spring is higher than the inland freshwater boundary.  
750 The mixing zone position also keeps moving landward slowly and persistently.  
Compared with the maximum seawater intrusion benchmark with a stress period of 7-day  
elapsed time in simulation, the mixing zone position after the 14-day simulation moves  
additional 1.29 km landward in the conduit and the surrounding porous medium. In the  
prediction of SEAWAT model, the mixing zone finally moves to 7.56 (7.89) km from the  
755 shoreline after the 21 (28)-day extended low rainfall period. Above all, seawater keeps  
intruding further inland through conduit network during an extended low rainfall period.



In such condition, the contamination of fresh groundwater resources in the aquifer becomes an environmental issue in coastal regions.



## 760 6. Summary and Conclusion

In this study, a 2D SEAWAT model is developed to evaluate the parameter sensitivities and quantitatively estimate seawater intrusion in a dual-permeability coastal karst aquifer with a conduit network. In the local sensitivities analysis, the composite scaled sensitivities (CSS) are calculated to assess the salinity and head simulations in the conduit and the porous medium at specified parameter values. Salinity at the submarine spring (SC) is identified as the most important parameter to the simulations in both two domains, because the submarine spring is the major entrance of seawater intrusion into the conduit as pathway in the aquifer. The boundary conditions and hydrological characteristics of the conduit, including sea level at the submarine spring (H\_SL),


765 hydraulic conductivity (HY\_C) and effective porosity (PO\_C) are important to the simulations in the conduit as well. On the other hand, the simulations in the porous medium also are sensitive to the boundary conditions (SC and H\_SL) and hydrological characteristics of the conduit, such as specific storage and effective porosity (SS\_C and PO\_C), due to the interaction and exchange between the two domains. Sensitivity


770 analysis indicates that the observations and simulations in the conduit are especially important for understanding hydrogeological processes and modeling seawater intrusion in such a dual-permeability karst aquifer. In addition, the largest CSS values of parameter sensitivities can be found around the mixing zone position. The local sensitivity analysis in this study confirms the conclusions of sensitivity studies in a homogeneous aquifer in





780 Shoemaker (2004), also highlights the values of conduit network in modeling seawater intrusion in a coastal karst aquifer.

The global sensitivity analysis indicates that head simulation in the conduit is more sensitive to effective porosity (PO\_C) and specific storage of the conduit (SS\_C), instead of hydraulic conductivity. The conduit flow easily becomes non-laminar and  
785 beyond the capability of Darcy equation in SEAWAT model, which assumes a linear relationship between specific discharge and head gradient. Therefore, the uncertainty of conduit permeability is difficult to be accurately evaluated by hydraulic conductivity in the continuum model. Different from the local sensitivity study, hydraulic conductivity of the porous medium (HY\_P) has the largest mean of EEs with respect to head 

790 simulation in the porous medium **Simulations** are non-linear to parameter SC, which has the largest derivative in the ified evaluated location in the local sensitivity study., Dispersivity is no longer an important parameter for simulations in the conduit, which is different from Shoemaker (2004), because advection is dominated in the solution of saline water transport with turbulent flow in the conduit, as well as the relatively fast  
795 seepage flow in the surrounding porous medium. In the salinity profile, the mixing is mostly due to numerical dispersion instead of the solution of dispersion equation, since Peclet number is extremely large and beyond the criteria of solving transport equation by finite difference method.

Seawater intrusion is quantitatively estimated with variations of salinity and sea  
800 level at the submarine spring, which are identified as important parameters in sensitivity study. Seawater intrudes significantly further landward through the conduit, and flows into the surrounding porous medium via the exchange on the pipe wall. Salinity and head



boundary conditions of 35.0 PSU and 0.0 m, respectively, are set at the submarine spring  
in the case of the maximum seawater intrusion. The mixing zone position in the conduit  
805 moves to 5.80 km from the shoreline with 1.13 km wide after a 7-day low rainfall period.  
Rainfall and regional recharges dilute the salinity at the submarine spring (SC), and  
significantly shift the mixing zone position seaward to 4.0 (4.5) km away from the  
shoreline with salinity of 10.0 (20.0) PSU. Compared with the benchmark, seawater  
intrudes additional 1.29 (2.25) km further landward along the conduit under 0.91 (1.82)  
810 m sea level rise at the submarine spring (H\_SL). In addition, the impacts of an extended  
low rainfall period on seawater intrusion through conduit network are also quantitatively  
assessed with longer elapsed time in simulation. The mixing zone position moves to 7.56  
(7.89) km from the shoreline, after a 21 (28)-day low precipitation period.

In a summary, the conduit network is important as the major pathway for seawater  
815 intrusion in the aquifer, and the submarine spring is the major entrance of seawater  
intrusion into the conduit. Some parameters, such as dispersivity and hydraulic  
conductivity in the conduit, have different sensitivities from the previous studies for a  
homogeneous aquifer. More attentions on the modeling and field observations in the  
karst features, including the subsurface conduit network, the submarine spring and karst  
820 windows, are meaningful and important for calibrating the model and for understanding  
seawater intrusion in a coastal karst aquifer.



### Competing interests

The authors declare that they have no conflict of interest.

825



## References

- Bear, J.: Seawater intrusion in coastal aquifers, Springer Science & Business Media, 1999.
- Calvache, M., and Pulido-Bosch, A.: Effects of geology and human activity on the  
830 dynamics of salt-water intrusion in three coastal aquifers in southern Spain,  
Environmental Geology, 30, 215-223, 1997.
- Custodio, E.: Salt-fresh water interrelationships under natural conditions, Groundwater  
Problems in Coastal Areas, UNESCO Studies and Reports in Hydrology, 45, 14-96,  
1987.
- 835 Davis, J. H.: Hydraulic investigation and simulation of ground-water flow in the Upper  
Floridan aquifer of north central Florida and southwestern Georgia and delineation of  
contributing areas for selected City of Tallahassee, Florida, Water-Supply Wells, U.S.  
Geological Survey, Tallahassee, Florida, 55, 1996.
- Davis, J. H., and Katz, B. G.: Hydrogeologic investigation, water chemistry analysis, and  
840 model delineation of contributing areas for City of Tallahassee public-supply wells,  
Tallahassee, Florida, Geological Survey (US)2328-0328, 2007.
- Davis, J. H., Katz, B. G., and Griffin, D. W.: Nitrate-N movement in groundwater from  
the land application of treated municipal wastewater and other sources in the Wakulla  
Springs Springshed, Leon and Wakulla counties, Florida, 1966–2018, US Geol Surv Sci  
845 Invest Rep, 5099, 90, 2010.
- Davis, J. H., and Verdi, R.: Groundwater Flow Cycling Between a Submarine Spring and  
an Inland Fresh Water Spring, Groundwater, 52, 705-716, 2014.
- Diersch, H.: FEFLOW reference manual, Institute for Water Resources Planning and  
Systems Research Ltd, 278, 2002.
- 850 Essink, G., Van Baaren, E., and De Louw, P.: Effects of climate change on coastal  
groundwater systems: a modeling study in the Netherlands, Water Resources Research,  
46, 2010.
- Fleury, P., Bakalowicz, M., and de Marsily, G.: Submarine springs and coastal karst  
aquifers: a review, Journal of Hydrology, 339, 79-92, 2007.



- 855 Gallegos, J. J., Hu, B. X., and Davis, H.: Simulating flow in karst aquifers at laboratory and sub-regional scales using MODFLOW-CFP, *Hydrogeology Journal*, 21, 1749-1760, 2013.
- Guo, W., and Langevin, C.: User's guide to SEWAT: a computer program for simulation of three-dimensional variable-density ground-water flow, *Water Resources Investigations Report*. United States Geological Survey, 2002.
- 860 Hill, M. C., and Tiedeman, C. R.: Effective groundwater model calibration: with analysis of data, sensitivities, predictions, and uncertainty, John Wiley & Sons, 2006.
- Inouchi, K., Kishi, Y., and Kakinuma, T.: The motion of coastal groundwater in response to the tide, *Journal of Hydrology*, 115, 165-191, 1990.
- 865 IPCC: Contribution of Working Groups I, II and III to the Fourth Assessment Report of the Intergovernmental Panel on Climate Change, Geneva, Switzerland, 104 pp., 2007.
- Kernagis, D. N., McKinlay, C., and Kincaid, T. R.: Dive Logistics of the Turner to Wakulla Cave Traverse, 2008.
- Kincaid, T. R., and Werner, C. L.: Conduit Flow Paths and Conduit/Matrix Interactions Defined by Quantitative Groundwater Tracing in the Floridan Aquifer, Sinkholes and the Engineering and Environmental Impacts of Karst: Proceedings of the Eleventh Multidisciplinary Conference, *Am. Soc. of Civ. Eng. Geotech. Spec. Publ*, 2008, 288-302,
- 870 Langevin, C. D., Shoemaker, W. B., and Guo, W.: MODFLOW-2000, the US Geological Survey Modular Ground-Water Model--Documentation of the SEAWAT-2000 Version with the Variable-Density Flow Process (VDF) and the Integrated MT3DMS Transport Process (IMT), US Department of the Interior, US Geological Survey, 2003.
- Martin, J. B., and Dean, R. W.: Exchange of water between conduits and matrix in the Floridan aquifer, *Chemical Geology*, 179, 145-165, 2001.
- 880 Martin, J. B., Gulley, J., and Spellman, P.: Tidal pumping of water between Bahamian blue holes, aquifers, and the ocean, *Journal of Hydrology*, 416, 28-38, 2012.
- Moore, W. S., and Wilson, A. M.: Advective flow through the upper continental shelf driven by storms, buoyancy, and submarine groundwater discharge, *Earth and Planetary Science Letters*, 235, 564-576, 2005.



- 885 Morris, M. D.: Factorial sampling plans for preliminary computational experiments,  
Technometrics, 33, 161-174, 1991.
- Poeter, E. P., and Hill, M. C.: Documentation of UCODE, a computer code for universal  
inverse modeling, DIANE Publishing, 1998.
- Reimann, T., Liedl, R., Giese, M., Geyer, T., Maréchal, J.-C., Dörfli, N., Bauer, S.,  
890 and Birk, S.: Addition and Enhancement of Flow and Transport processes to the  
MODFLOW-2005 Conduit Flow Process, 2013 NGWA Summit—The National and  
International Conference on Groundwater, 2013,
- Reimann, T., Giese, M., Geyer, T., Liedl, R., Maréchal, J.-C., and Shoemaker, W. B.:  
Representation of water abstraction from a karst conduit with numerical discrete-  
895 continuum models, Hydrology and Earth System Sciences, 18, 227-241, 2014.
- Saltelli, A., Tarantola, S., Campolongo, F., and Ratto, M.: Sensitivity analysis in practice:  
a guide to assessing scientific models, John Wiley & Sons, 2004.
- Shoemaker, W. B.: Important observations and parameters for a salt water intrusion  
model, Ground Water, 42, 829-840, 2004.
- 900 Shoemaker, W. B., Kuniandy, E. L., Birk, S., Bauer, S., and Swain, E. D.:  
Documentation of a conduit flow process (CFP) for MODFLOW-2005, 2008.
- Voss, C. I., and Provost, A. M.: SUTRA, US Geological Survey Water Resources  
Investigation Reports, 84-4369, 1984.
- Voss, C. I., and Souza, W. R.: Variable density flow and solute transport simulation of  
905 regional aquifers containing a narrow freshwater - saltwater transition zone, Water  
Resources Research, 23, 1851-1866, 1987.
- Werner, A. D., and Simmons, C. T.: Impact of sea - level rise on sea water intrusion in  
coastal aquifers, Groundwater, 47, 197-204, 2009.
- Werner, A. D., Bakker, M., Post, V. E., Vandenbohede, A., Lu, C., Ataie-Ashtiani, B.,  
910 Simmons, C. T., and Barry, D. A.: Seawater intrusion processes, investigation and  
management: recent advances and future challenges, Advances in Water Resources, 51,  
3-26, 2013.
- WHO: Guidelines for Drinking-water Quality, 104-108, 2011.





- Wilson, A. M., Moore, W. S., Joye, S. B., Anderson, J. L., and Schutte, C. A.: Storm -  
915 driven groundwater flow in a salt marsh, *Water Resources Research*, 47, 2011.
- Xu, Z., Hu, B. X., Davis, H., and Cao, J.: Simulating long term nitrate-N contamination  
processes in the Woodville Karst Plain using CFPv2 with UMT3D, *Journal of  
Hydrology*, 524, 72-88, 2015a.
- Xu, Z., Hu, B. X., Davis, H., and Kish, S.: Numerical study of groundwater flow cycling  
920 controlled by seawater/freshwater interaction in a coastal karst aquifer through conduit  
network using CFPv2, *Journal of contaminant hydrology*, 182, 131-145, 2015b.
- Xu, Z., Bassett, S. W., Hu, B., and Dyer, S. B.: Long distance seawater intrusion through  
a karst conduit network in the Woodville Karst Plain, Florida, *Scientific Reports*, 6, 2016.
- Xu, Z., and Hu, B. X.: Development of a discrete - continuum VDFST - CFP numerical  
925 model for simulating seawater intrusion to a coastal karst aquifer with a conduit system,  
*Water Resources Research*, 53, 688-711, 10.1002/2016WR018758., 2017.



Table 1. The symbols and definitions of parameters used in this study, the specified evaluated values in local sensitivity study and evaluation ranges (the lower and upper constraints) of each parameter in global sensitivity analysis.

Parameter	Definitions	Lower	Upper	Evaluated value	Unit
HY_P	Hydraulic conductivity (porous medium)	1.524	4.572	2.286	meter/day ( $\times 10^3$ )
HY_C	Hydraulic conductivity (conduit)	3.048	9.144	6.096	meter/day ( $\times 10^5$ )
SS_P	Specific storage (porous medium)	4.00	6.00	5.00	dimensionless ( $\times 10^{-7}$ )
SS_C	Specific storage (conduit)	0.03	0.07	0.05	dimensionless
RCH	Recharge rate on the surface	0.00	0.03	0.01	meter/day
H_SL	Sea level at the submarine spring	-0.305	0.914	0.305	meter
PO_P	Porosity (porous medium)	0.001	0.005	0.003	dimensionless
PO_C	Porosity (conduit)	0.200	0.400	0.300	dimensionless
SC	Salinity at the submarine spring	0.0	35.0	35.0	PSU
DISP_P	Longitudinal dispersivity (porous medium)	6.10	12.20	10.00	meter
DISP_C	Longitudinal dispersivity (conduit)	0.15	0.60	0.30	meter

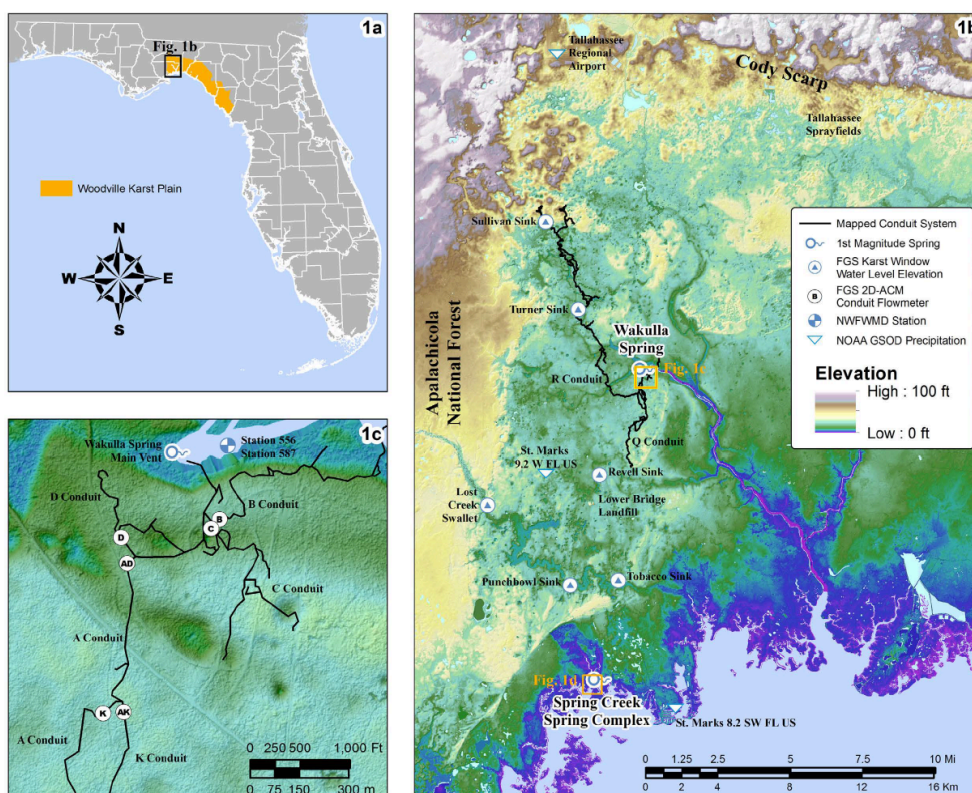


Figure 1. a) Locations of the Woodville Karst Plain (WKP) and the study site; b) The map of the Woodville Karst Plain showing the locations of features of note with the study; c) The detail of cave system near Wakulla Springs. Modified from Xu et al., (2016).

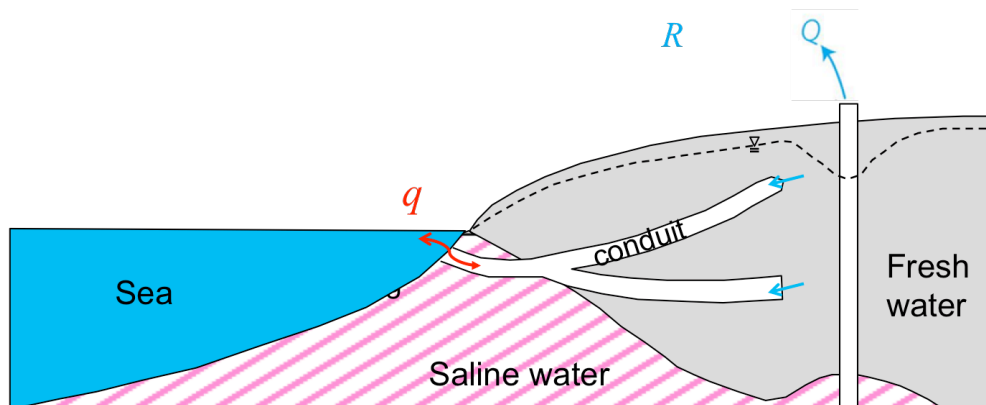
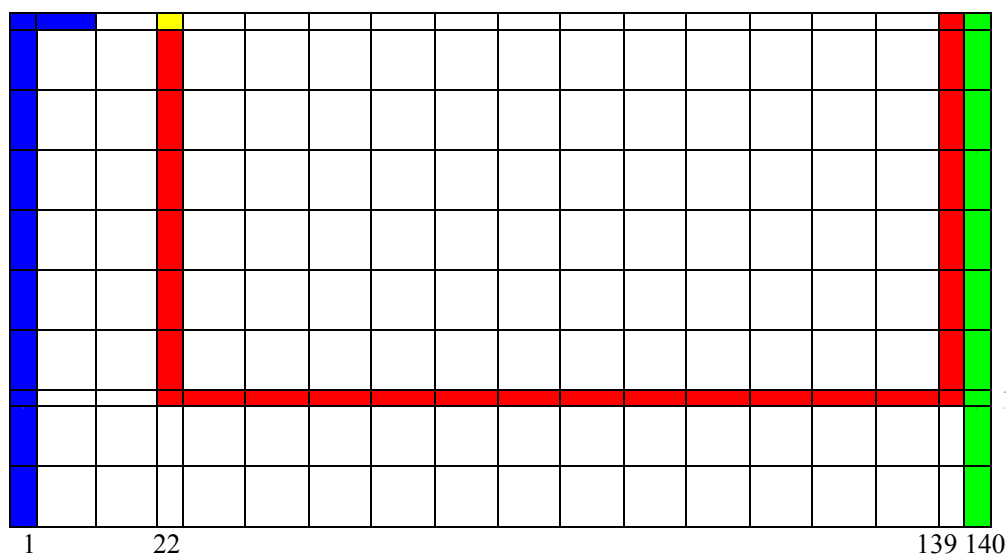


Figure 2. Schematic figure of a coastal karst aquifer with conduit networks and a submarine spring opening to the sea in a cross section. Flow direction  $q$  would be seaward when sea level drops, pumping rate  $Q$  is low and precipitation recharge  $R$  is large; however, reversal flow occurs when sea level rises, pumping rate  $Q$  is high or precipitation recharge  $R$  is small.



Explanations:

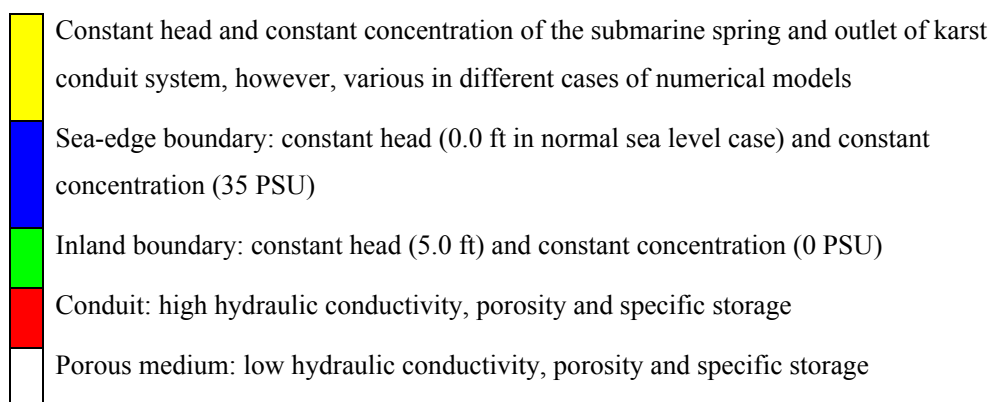


Figure 3. Schematic figure of finite difference grid discretization and boundary conditions applied in the SEAWAT model. Every cell represents 10 horizontal cells and 4 vertical cells, except the boundary and conduit layer in color with smaller width. The submarine spring is located at column #22, layer #1, and the inland spring is located at column #139, layer #1. The conduit system starts from the top of column #22, descends downward to layer #29, horizontally extends to column #139, and then rises upward to the top through column #139.

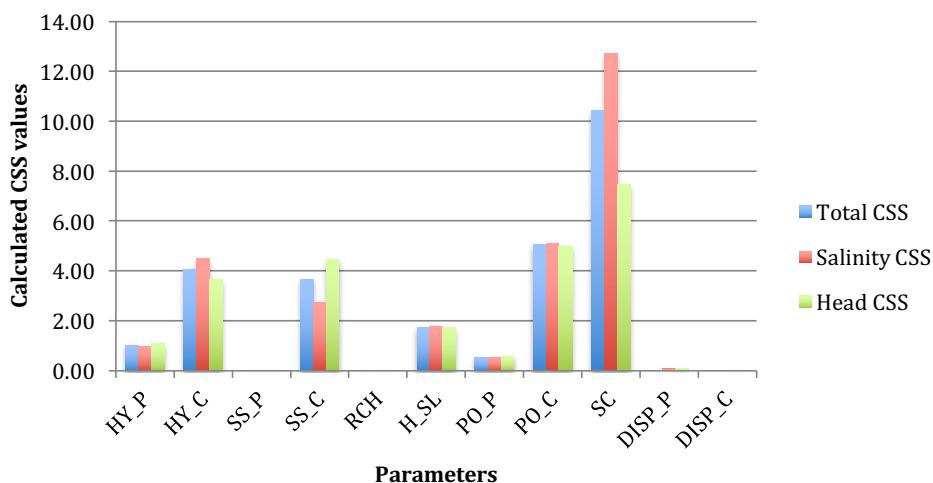


Figure 4. The CSSs (Composite Scaled Sensitivities) of all parameters with respect to simulations in the conduit (layer #29) in the local sensitivity analysis.

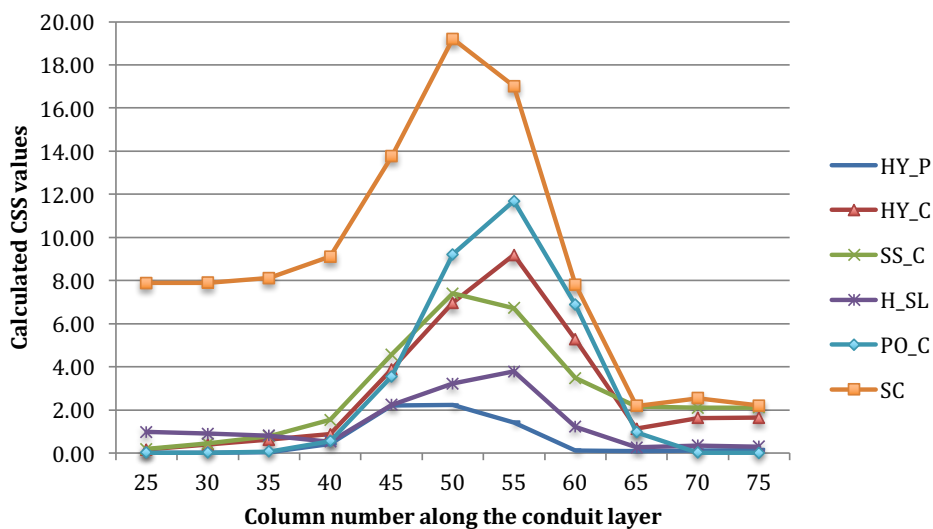


Figure 5. The CSSs (Composite Scaled Sensitivities) of selected parameters at different locations along the conduit layer (from column #25 to column #75) in the local sensitivity analysis.

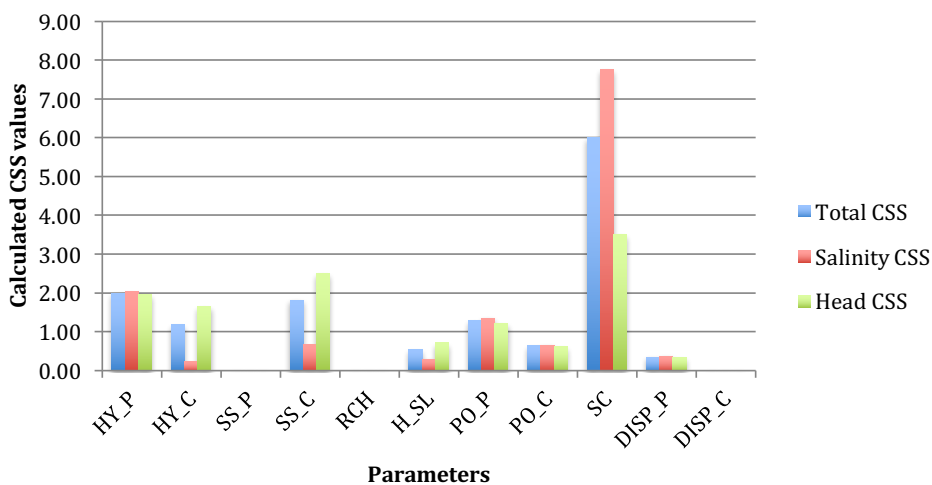


Figure 6. The CSSs (Composite Scaled Sensitivities) of all parameters with respect to simulations in the porous medium (layer #24) in the local sensitivity analysis.

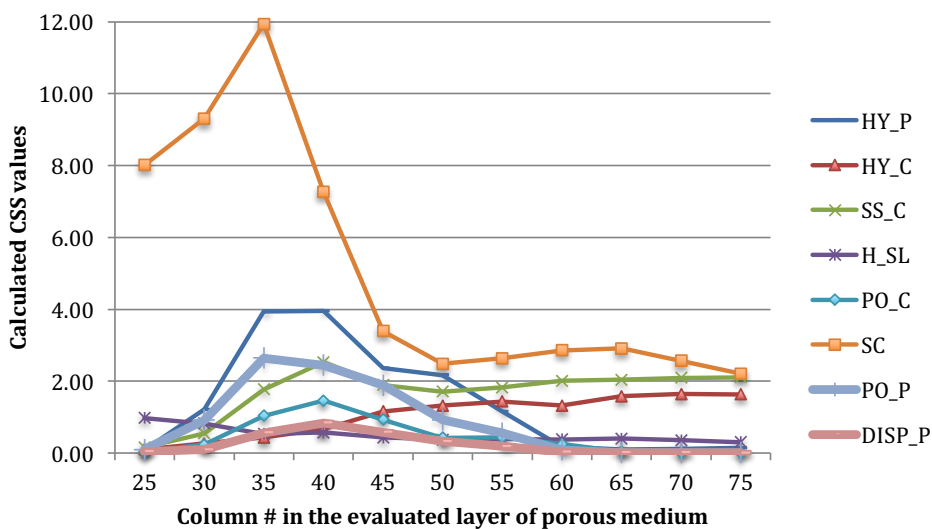


Figure 7. The CSSs (Composite Scaled Sensitivities) at different locations in the porous medium (from column #25 to column #75 at layer # 24) in the local sensitivity analysis.

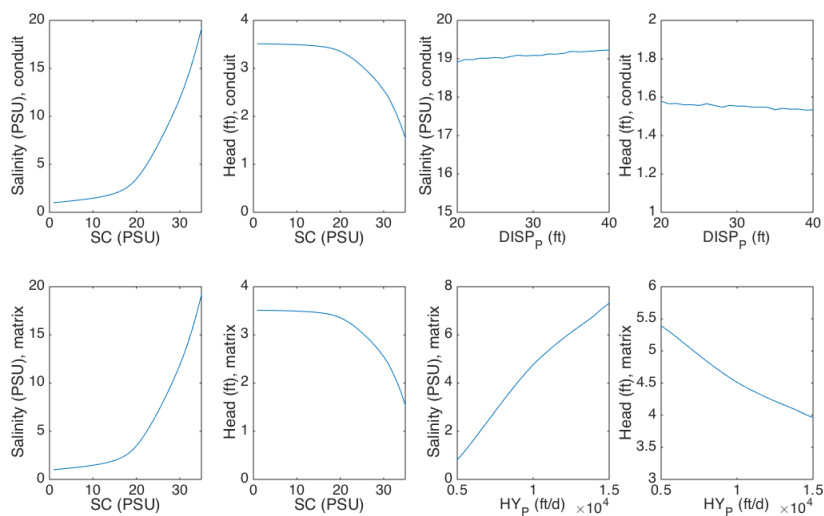


Figure 8. The non-linear relationship between head and salinity simulations with respect to parameters SC, DISP\_P and HY\_P. (Note that the scale for each plot is different).



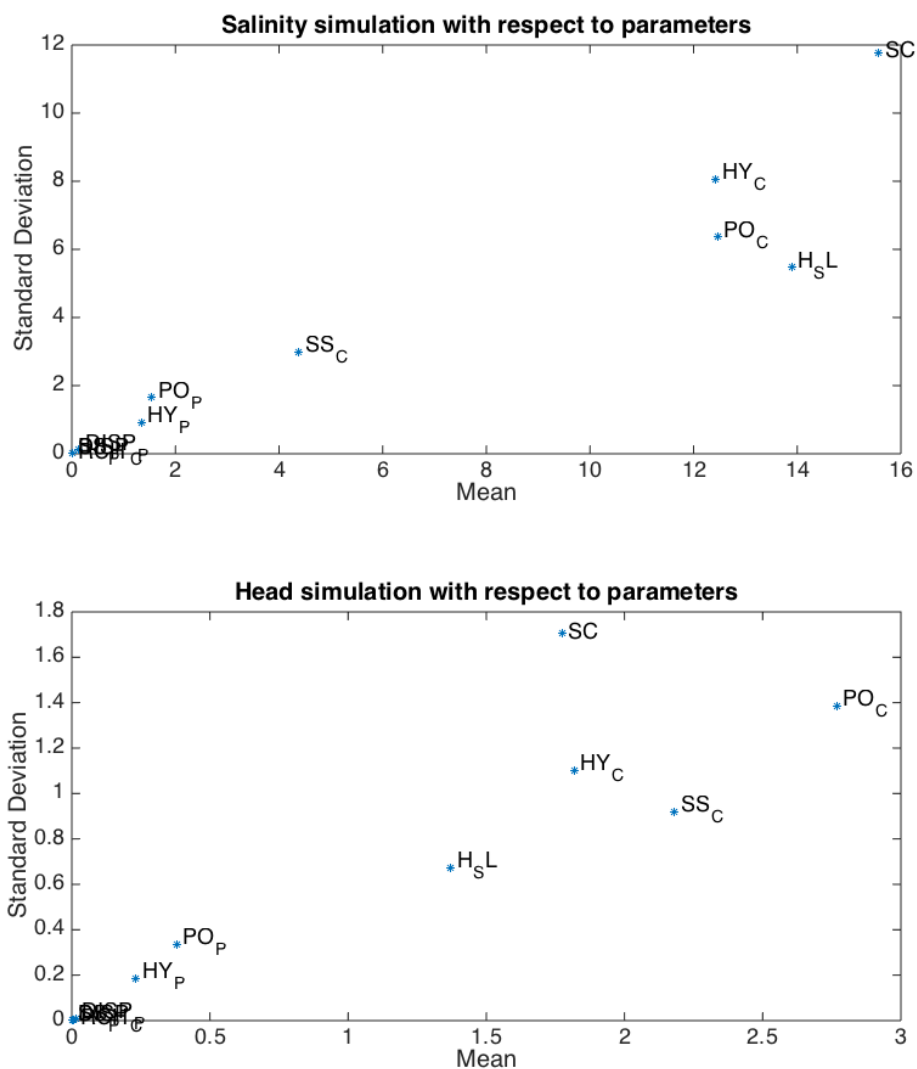


Figure 9. Mean and standard deviation of the EEs (elementary effects) of parameters with respect to simulations in the conduit (column #50, layer #29) by the trajectory sampling Morris method in the global sensitivity analysis: a) salinity simulation (top); b) head simulation (bottom).

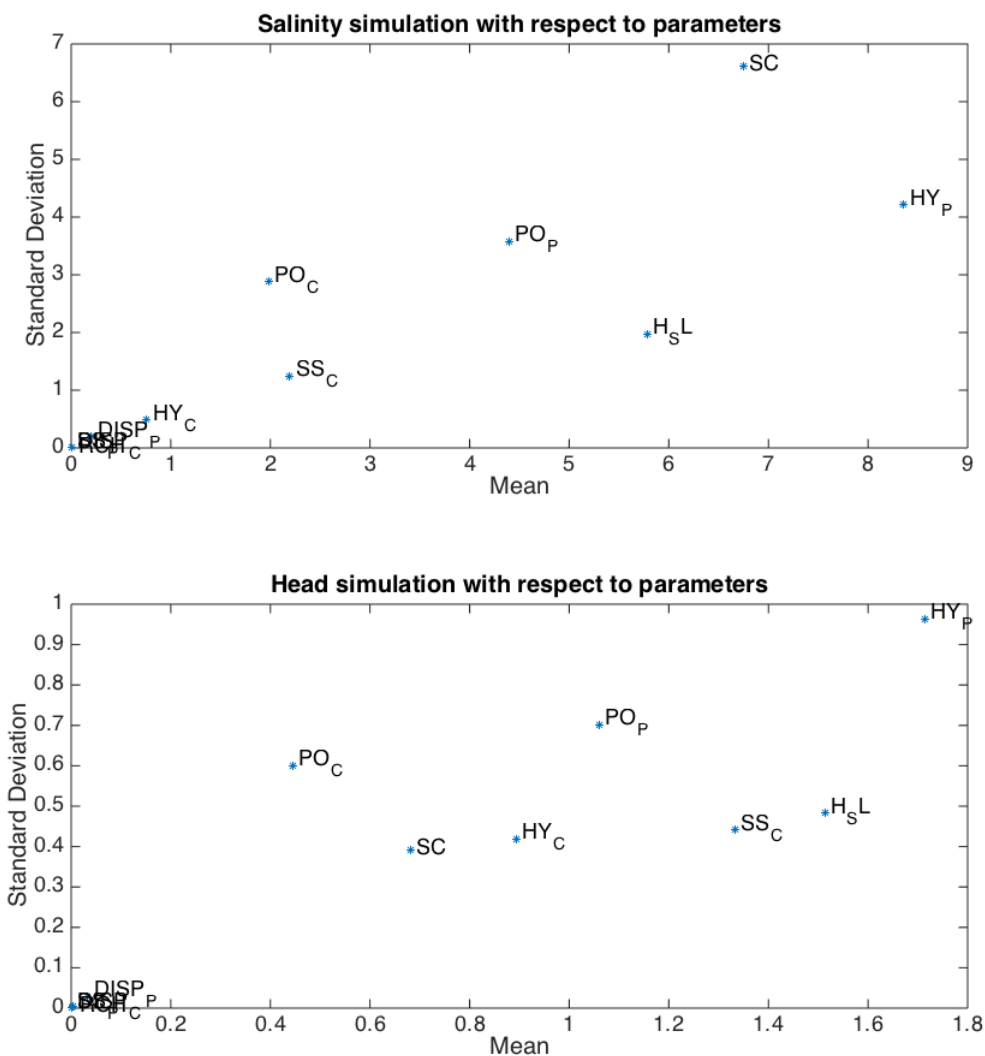


Figure 10. Mean and standard deviation of the EEs (elementary effects) of parameters with respect to simulations in the porous medium (column #35, layer #24) by trajectory sampling Morris method in the global sensitivity analysis: a) salinity simulation (top); b) head simulation (bottom).

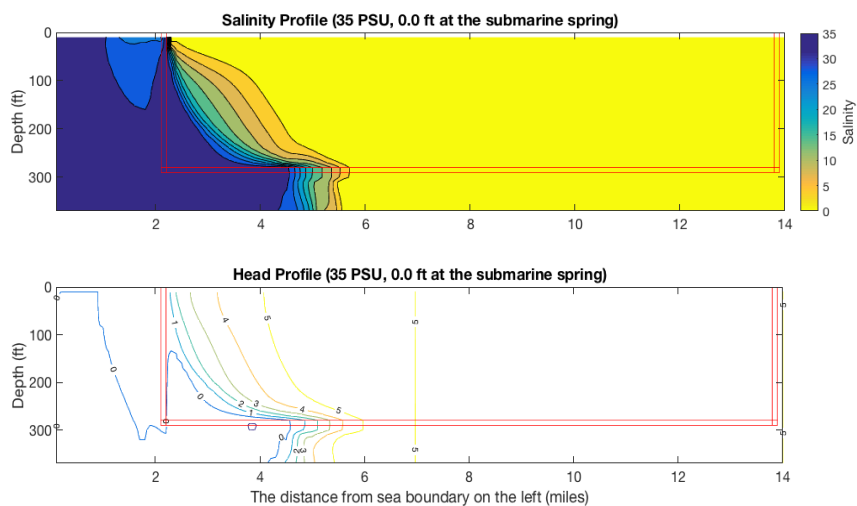


Figure 11. Salinity (top) and head (bottom) simulations of the maximum seawater intrusion case (35 PSU, 0.0 ft at the submarine spring).

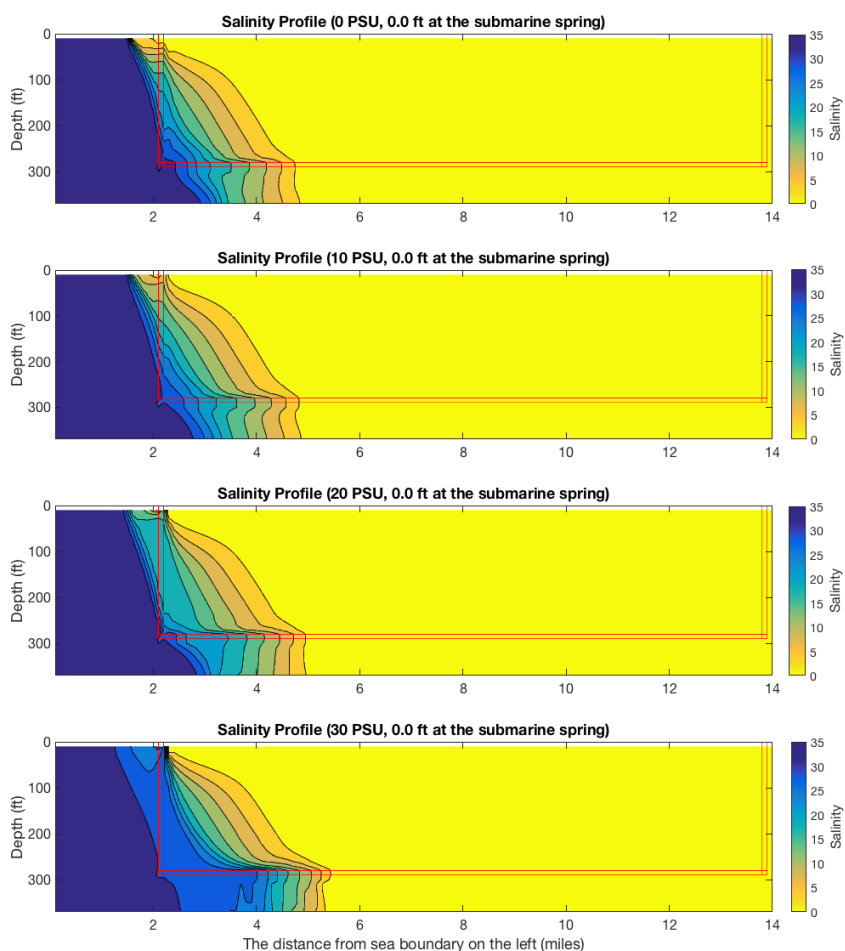


Figure 12. Salinity simulation of seawater intrusion with various salinity at the submarine spring, indicating different rainfall recharge and freshwater discharge conditions: A) 0.0 PSU, 0.0 ft at the submarine spring; B) 10.0 PSU, 0.0 ft at the submarine spring; C) 20.0 PSU, 0.0 ft at the submarine spring; D) 30.0 PSU, 0.0 ft at the submarine spring (from top to bottom).

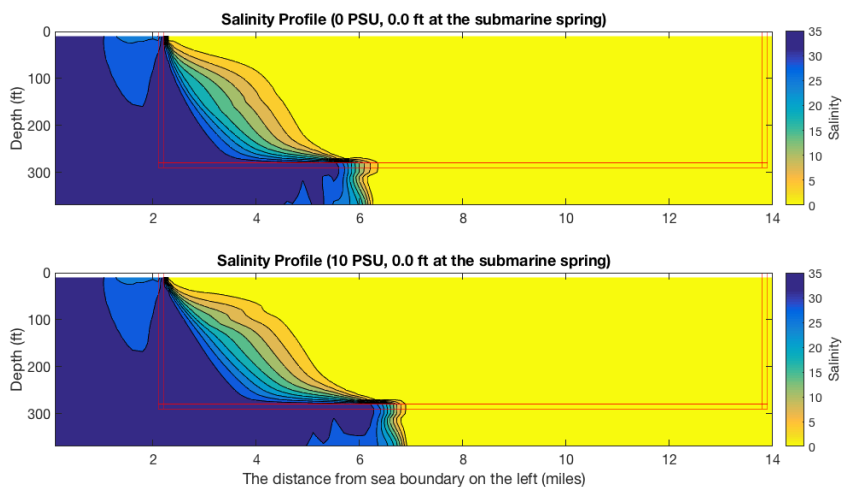


Figure 13. Salinity simulation of seawater intrusion with various sea level conditions: A) 35.0 PSU, 3.0 ft at the submarine spring; B) 35.0 PSU, 6.0 ft at the submarine spring (from top to bottom).

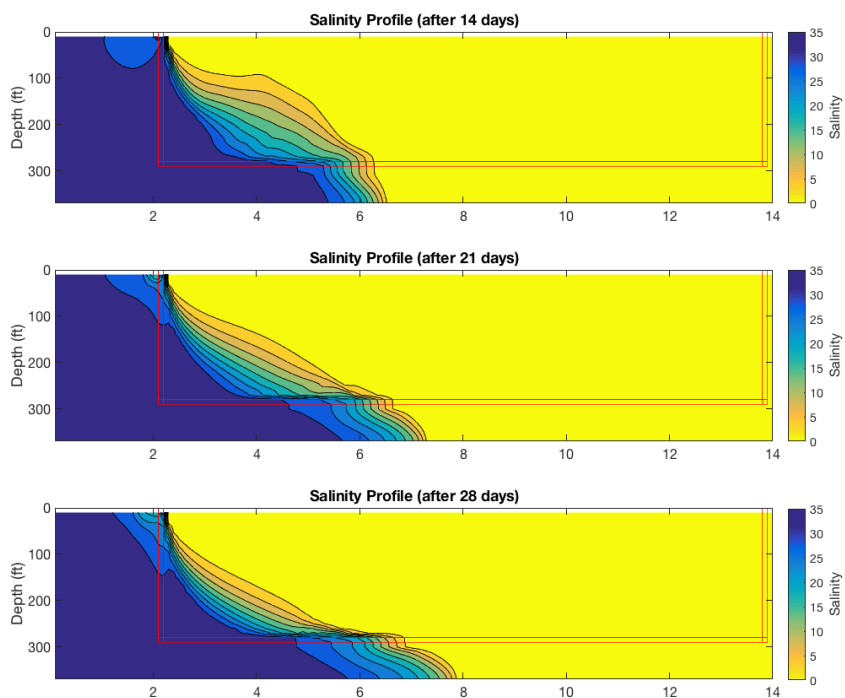


Figure 14. Salinity simulation of the maximum seawater intrusion case (35 PSU, 0.0 ft at the submarine spring) with extend simulation time during a low rainfall period: A) 14-day simulation period; B) 21-day simulation period; C) 28-day simulation period (from top to bottom).